University Turbine Systems Research (UTSR)

2018 Gas Turbine Industrial Fellowship Program

Final Report

Prepared by:

Thomas Glenn

B.S. Aerospace Engineering Candidate

Georgia Institute of Technology

Prepared for:

Southwest Research Institute

6220 Culebra Road

San Antonio, TX 78238

1. Introduction

The University Turbine Systems Research (UTSR) program offers university research students with the opportunity to gain experience in industrial gas turbine design and manufacturing. Southwest Research Institute (SwRI) manages and participates in this program, offering research fellows access to the broad scope of skills and knowledge within SwRI's Mechanical Engineering department, Division 18. SwRI has decades of experience with gas turbine and rotating machinery systems. This report will outline several tasks performed as part of this fellowship, namely the design and construction of an axial compressor test demo, a review of high-pressure oxygen safety considerations, and assistance in restarting work on the Great Horned Owl program, an original gas turbine design.

2. Axial Compressor Test Demo

2.1. Background

SwRI offers a variety of training courses in turbomachinery design, so a need was identified for an axial compressor test stand for use as a training demo. The stand will provide examples in aerodynamic design and compressor performance. The design should be simple enough to allow for hand-calculations in a classroom setting. Additionally, the test stand is self-contained and portable, allowing the demo to be easily transported as needed.

2.2. Design

The most vital component of an axial compressor demo is naturally the compressor itself. Prior to the beginning of this fellowship, SwRI had obtained a cordless leaf blower featuring a two-stage axial compressor. The blower is shown in Figure 1. Note the compressor stages seen in the transparent middle section.

Figure 1. Axial blower used in demo

As manufactured, the blower throttle is controlled through a trigger. However, this does not allow for stable output. To remedy this, the trigger is replaced by a potentiometer of

comparable resistance. The manufacturer lists the following performance specifications of the blower:

Air Volume Flow Rate	Air Speed (Peak)	Air Speed (Average)
450/545 cfm	90/125 mph	75/100 mph
12/15 m3/min	145/200 km/h	120/160 km/h

Table 1. Blower performance specifications

In addition to having steady flow, the output from the blower must be guided through piping and instrumentation in order to measure useful data. Figure 2 shows a rough planning schematic of the test rig.

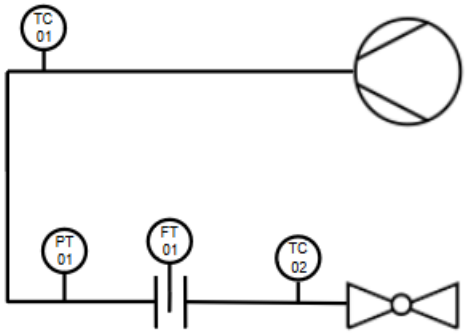

Figure 2. Piping and instrumentation diagram of axial compressor test demo

The blower, piping, and instrumentation are all mounted on a 36” x 48” x 50” wooden display cart with wheels for easy transportation. The test rig uses a 0-50 in. H_2O differential pressure sensor and a 0-10 in. H_2O static pressure sensor. The finished test stand can be seen in Figure 3 below.

Figure 3. Mounted axial compressor test demo

2.3. Calculations and Modeling

An orifice plate with is used to measure mass flow rate (q_m) using the following formula (ASME MFC-3M-1989) :

$$q_m = \frac{\pi}{4} C \epsilon_1 d^2 \sqrt{\frac{2\Delta p \rho_{f_1}}{1-\beta^4}}, for\ metric\ units$$

An orifice plate diameter (*d)* is selected to be 2.3 inches with a pipe diameter of 3 inches. This results in a β ratio of approximately 0.76. Using sample calculations for orifice plates with a similar β ratio from ASME MFC-3M-1989, the discharge coefficient (*C)* is estimated to be 0.61. The flow is incompressible, so the expansibility factor (ϵ_1) is assumed to equal 1. Converting to metric units, the formula condenses to:

$$q_m = 0.00349597 \sqrt{\Delta p \rho_{f_1}}$$

Now, to solve for mass flow rate, all that is needed is the pressure drop (Δp) across the orifice plate and the density (ρ_{f_1}) of the fluid. This compressor demo is concerned with compressor performance, so a compressor map would prove a useful visual demonstration. For this, the pressure ratio *PR* must be determined:

$$PR = \frac{P_{out}}{P_{in}}$$

Plotting the pressure ratio against mass flow rate at varying conditions will populate the compressor map. A tachometer is used to measure the RPM range of the blower, allowing for the construction of a theoretical model of compressor performance. The model is built using a combination of the pressure/temperature relationship for isentropic compression and velocity triangles. Blade angles are used with the measured RPM values to determine the enthalpy rise across the compressor. The velocity triangles including measured rotor blade angles are shown in Figure 4. RPM values can be converted to blade linear velocity (*u)* based on blower geometry, which then allows for enthalpy rise (*Δh)* to be calculated.

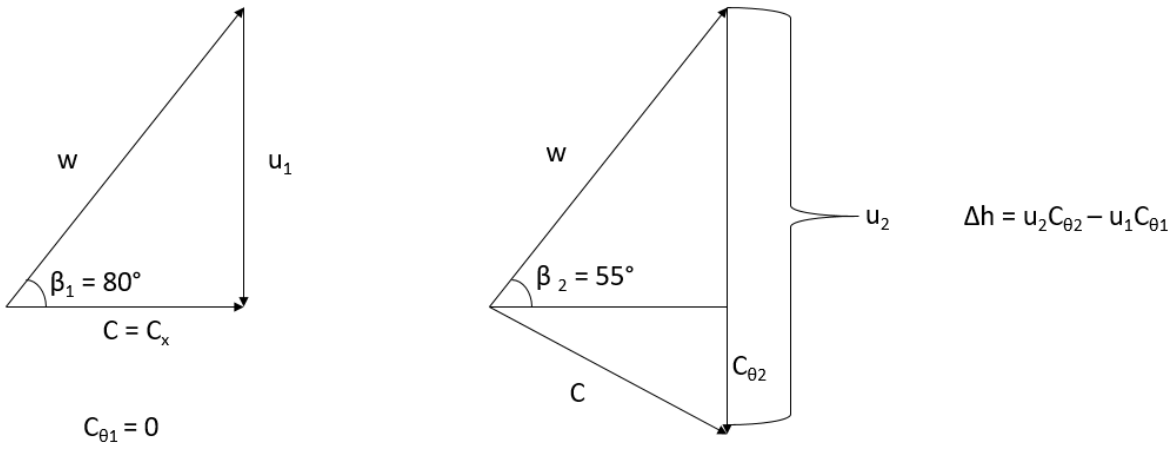

Figure 4. Velocity triangles (not to scale)

These enthalpy values are used as a benchmark to determine the pressure output from the compressor. The isentropic compression relationship below forms the basis of the model:

$$\frac{T_{out}}{T_{in}} = \left(\frac{p_{out}}{p_{in}}\right)^{1-\frac{1}{\gamma}}$$

The inlet pressure (p_{in}) and temperature (T_{in}) are assumed to be known, so in order to determine the pressure ratio, the compressor outlet temperature (T_{out}) must be solved for.

$$\Delta T = \frac{T_{out} - T_{in}}{\eta}$$

The model assumes an efficiency factor (η) of 70%. Knowing that $\Delta h = c_p \Delta T$, preliminary values for p_{out} are selected and tuned until the enthalpy rise is the same across both models. A model compressor map is constructed and shown in Figure 5.

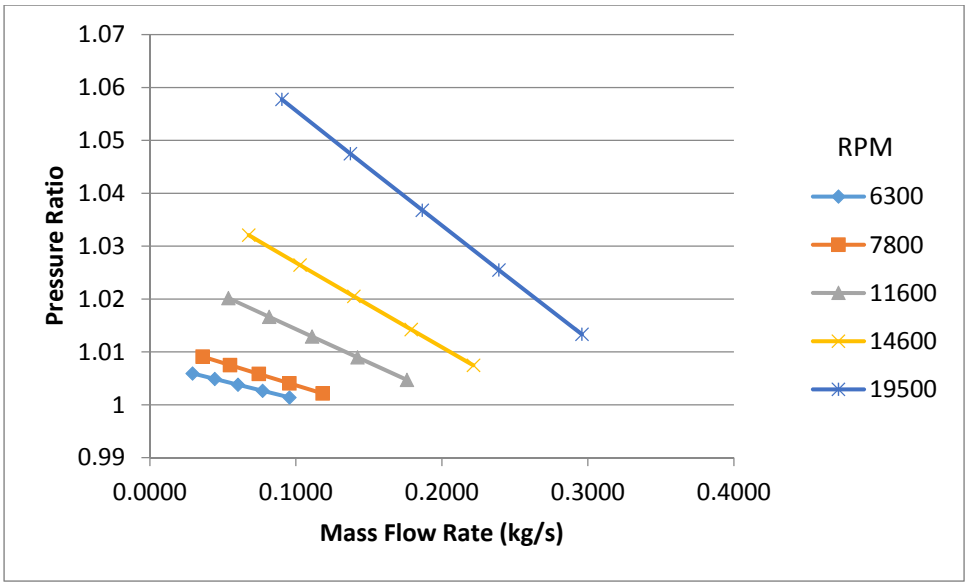

Figure 5. Theoretical compressor map of test demo

2.4. Experimental Data

Data is collected over a range of blower speeds and control valve settings. A compressor map of performance at speeds similar to the theoretical model is shown in Figure 6.

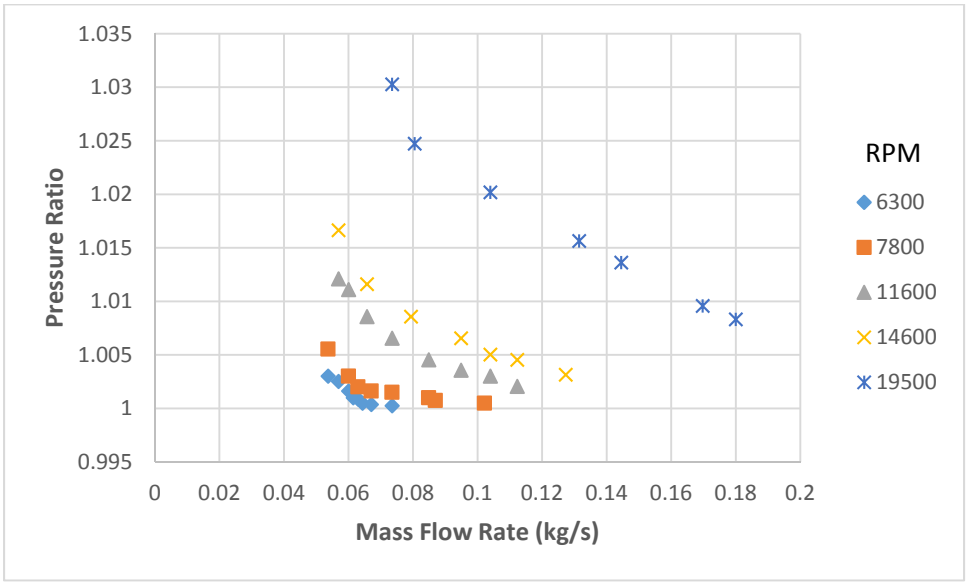

Figure 6. Compressor map of test demo using experimental data

The experimental data follows similar trends to the theoretical model, though it appears the blower's performance is roughly half that of the theoretical model. It should be noted that the theoretical model assumes isentropic compression, which is impossible for any real process. Additionally, the assumed isentropic efficiency could differ from actual

performance. Future work might improve upon the theoretical model to account for this discrepancy.

2.5. Conclusion and Future Development

Over the course of this fellowship, a functional test demo was constructed for use in SwRI demonstrations and technical courses. However, future work is required for a more robust demo. The pressure ratio produced by the blower is quite small, making it difficult to measure differential pressure across the orifice plate. A differential pressure range of 0 to 15 or 0 to 25 in. H_2O would produce more readable results, particularly for lower throttle settings. At higher blower speeds, vibrations made it difficult to read the gauges. Damping should be introduced to ensure more accurate measurements. Additionally, performance is highly dependent on blower battery charge. Over half of the battery charge was consumed in 30 minutes of testing, accompanied with a notable change in blower output at the same settings. An additional battery might be a worthwhile investment, particularly for classes where the test demo needs to be used over longer periods of time.

3. High-Pressure Oxygen Safety Review

3.1. Background

At high pressures, gaseous and liquid oxygen is an incredibly potent oxidizer. At 100% oxygen concentration, most nonmetals are flammable. As pressure is increased, metals will also become flammable. SwRI is currently developing an oxy-fuel supercritical CO_2 gas turbine combustor. At this stage in the project, a reduced flow test loop is being designed for combustor sub-component testing. A planning schematic of the testing setup is shown in Figure 7. The test loop will operate at reduced scale flow rates but will include high-pressure natural gas and oxygen supplies. Oxygen will be supplied at pressures as high as 31.6 MPa (4580 psi), requiring an investigation into high-pressure oxygen research in order to ensure safe design practices and operation procedures.

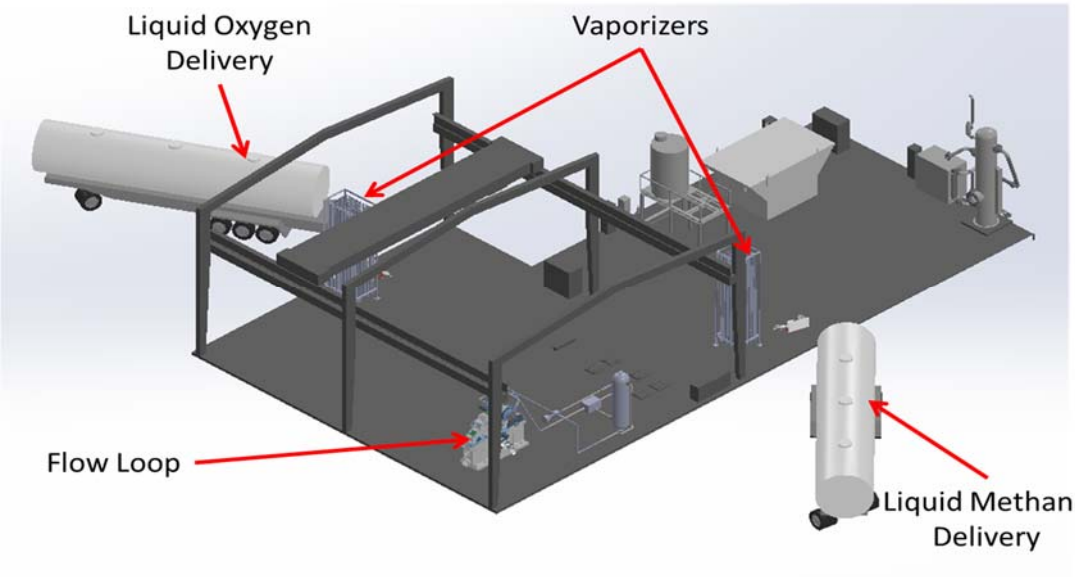

Figure 7. Reduced flow test loop layout

3.2. Oxygen Delivery Design

In order to supply high-pressure oxygen, liquid oxygen trailers will be connected to a cryogenic pump in order to achieve operating pressures up to 31.6 MPa. Flow exiting the pump will move through a vaporizer (and potentially a heater), followed by 50-100 feet of tubing, a flow meter, pressure/temperature instrumentation, and shutoff and control valves. Figure 8 shows an outline of this oxygen delivery system.

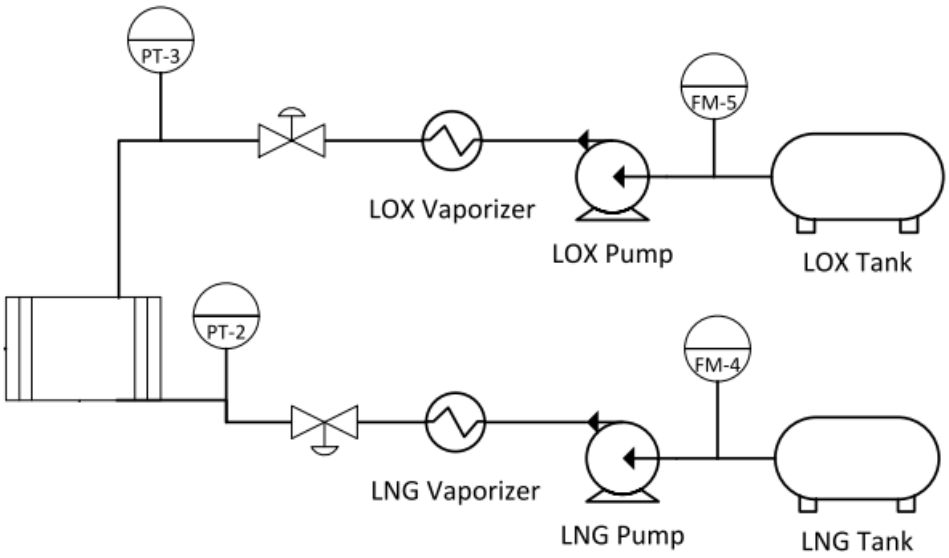

Figure 8. Piping and instrumentation diagram of LOX and LNG delivery

3.3. Oxygen Safety

High-pressure oxygen system safety concerns are highly dependent on component design and materials. Liquid oxygen is less likely to foster ignition due to lower temperatures, but risk still exists. Failure to account for increased risk of flammability can lead to potentially catastrophic damages and/or injuries. To mitigate risk, ignition hazards must be closely monitored and, if possible, eliminated.

3.3.1. Identification of Risk

The primary risk of high-pressure oxygen systems is ignition, which can be caused by a variety of mechanisms. Work by Beeson et al. lists the following as the primary sources of heat in oxygen systems: particle impact, heat of compression, flow friction, mechanical impact, friction, fresh metal exposure, static discharge, electrical arc, chemical reaction, thermal runaway, resonance, and external heat. Of these, the primary risk of ignition in the test loop oxygen delivery system is particle impact ignition caused by particles and contaminants that could become entrained in the flow. The risk of particle impact ignition can be reduced through proper selection of material and thorough cleaning (NSS 1740.15).

3.3.2. Material Safety

Selecting material for use in high-pressure oxygen systems can be challenging, as there is no single test applicable to all materials to determine ignition characteristics. Further, there is little recorded experience for oxygen at pressures above 20.7 MPa (NSS 1740.15). In general, nonmetals are extremely susceptible to spontaneous ignition in high-pressure oxygen. Thread lubricants, thread sealants, fluorocarbon plastics and elastomers, and tetrafluoroethylene (TFE) are considered high-risk components that can spontaneously ignite at temperatures between 200-500° C at 13.8-51.7 MPa (Nihart et al.). Therefore, all nonmetal components should be carefully selected and tested before use in oxygen applications. Metals are more resistant to ignition, but should still be selected carefully, particularly at high pressures and temperatures. ASTM G94.36237 provides in-depth material properties related to metal combustion in oxygen-rich environments. Experimental results show that nickel, Monel, brass, and Inconel are the most resistant to ignition, while stainless steel and aluminum are much easier to ignite. Despite this, stainless steel can still be used in oxygen systems and

there is extensive data available regarding safe operating parameters. Figures 9 and 10 depict safe operating pressures for carbon steel at 150° C and 200° C for stainless steel for impingement and non-impingement.

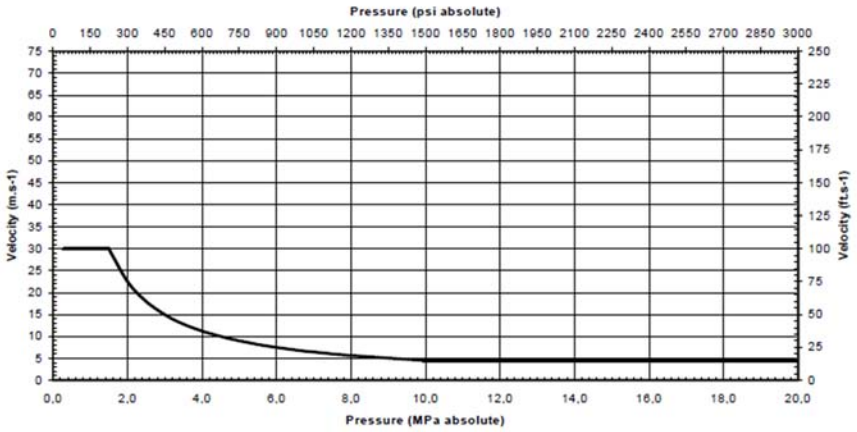

Figure 9. Impingement velocity curve for carbon steel at 150° C and stainless steel at 200° C (IGC Doc 13/12/E)

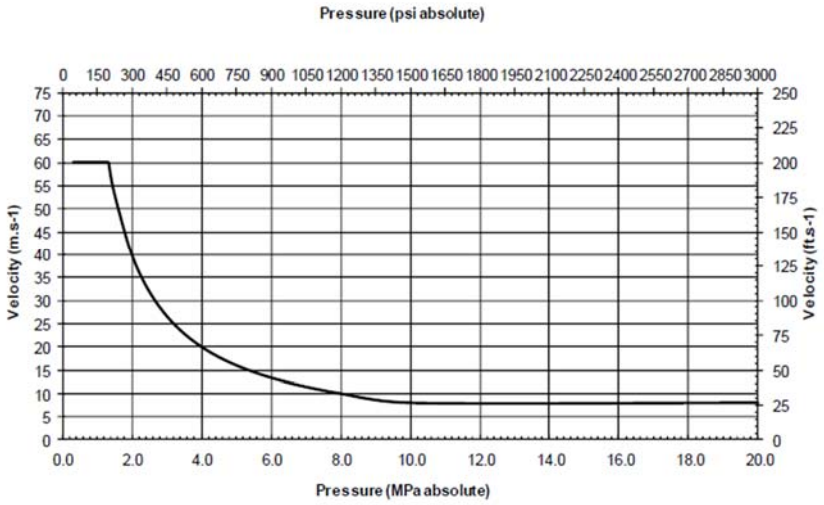

Figure 10. Non-impingement velocity curve for carbon steel at 150° C and stainless steel at 200° C (IGC Doc 13/12/E)

As shown by these two figures, acceptable flow velocity decreases rapidly as pressure is increased. Data is limited past 20.7 MPa, so if stainless or carbon steel is to be used at higher pressures, case-by-case material testing is highly recommended.

3.3.3. Component Safety

There are several high-risk components that should be closely analyzed when designing high-pressure oxygen systems. Valves in particular introduce a multitude of potential

ignition mechanisms to oxygen systems. Globe valves and butterfly valves are susceptible to impingement when fully open, which could potentially lead to particle impact ignition. Check valves and relief valves can introduce chattering, causing frictional heating or mechanical impact ignition. Ball valves are can generate particulate, potentially entraining material in the flow and causing particle impact ignition. Other items of risk include regulators, filters, and fittings (Stoltzfus et al.). Due to the fine configuration of the material, filters should be constructed of burn resistant materials such as nickel, bronze, or Monel. Regardless of material chosen, filters are an area of high risk due to direct impingement and accumulation of debris and particles. Piping systems should possess isolation valves and relief valves composed of oxygen-compatible material. High flow velocities (approaching 30 m/s) require special design considerations including long-radius bends and minimal valve usage (Beeson et al.).

3.3.4. Cleaning

Given that particle impact ignition carries the highest risk for ignition in the reduced flow test loop, proper cleaning will help reduce failure and damage. Any type of particulate within components should be thoroughly removed. This includes loose scale, rust, dirt, mill scale, weld spatter, weld flux, and any other foreign particulate that may become entrained in flow (Beeson et al.). Chemical and mechanical cleaning methods followed by professional visual inspection are highly recommended.

3.4. Conclusions and Recommendations

While there is a large amount of data available for oxygen systems, very little information exists for high pressure systems. Since the desired pressures for this test loop are above those observed in literature, it is strongly recommended for SwRI to test high-risk components before use in the oxygen delivery system. Proper material selection should be observed. Metals such as Inconel, Monel, and other copper and nickel alloys are superior to stainless steel at extreme pressures. When selecting valves, fast-opening mechanisms and valves with metal-metal contact should be avoided to prevent ignition. Proper material and component selection coupled with proper cleaning will help ensure the safe operation of the reduced flow test loop’s oxygen delivery system.

4. Great Horned Owl Gas Turbine Generator

4.1. Background

The Great Horned Owl (GHO) program is an Intelligence Advanced Research Projects Activity (IARPA) program focused on the development of systems that can be utilized in a small UAV. As part of this program, SwRI has developed and produced a prototype of a small, lightweight gas turbine generator designed to be used in an electric hybrid propulsion system. This generator features a novel single disk radial flow design allowing for simple construction and lightweight, rugged design. The GHO also features a novel bearing lubrication system utilizing two peristaltic pumps (Cunningham et al.). The current iteration of the generator is shown in Figure 11. Note that due to the protected nature of this project images and details will be limited.

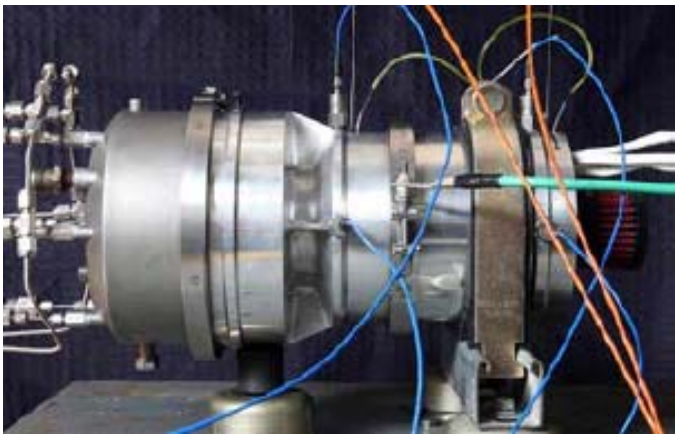

Figure 11. Generation 4 GHO design concept (Bryner et al.)

Until recently, the GHO project was on hold at SwRI, but the project has been renewed through an internal research and development project.

4.2. Build Tasks

As part of the renewal process, several tasks were undertaken as part of this fellowship, primarily focused on preparing the GHO for rotor balancing eventual combustor testing. Two computers were obtained for control and data acquisition. Vibration data is obtained using accelerometers connected to Alta software. Several parts had gone missing from the bearing lubrication system, so replacements had to be designed and installed. The bearings were visually inspected to ensure proper delivery of lubrication oil. A new fuel tank was also installed and connected to a boost pump supply. After installing bearing

thermocouples, the GHO was ready for rotor balancing. The rotor balancing process will occur after the completion of this fellowship.

5. Miscellanea

While the previous sections cover the primary tasks performed during this fellowship, several other smaller tasks were performed. Modal testing for a tie bolt rotor was performed, including ping testing and ANSYS analysis. A literature review on the relationship between axial preload and angular contact bearing stiffness was conducted, highlighting a strong disparity between experimental data and theoretical models.

6. Acknowledgements

I would like to thank UTSR and SwRI for the opportunity to participate in the 2018 Gas Turbine Industrial Fellowship Program. I would like to extend a special thanks to Klaus Brun, Tim Allison, David Ransom, Aaron Rimpel, Natalie Smith, Seth Cunningham, and Griffin Beck for providing me with opportunities to learn and develop valuable new skills.

Works Cited

ASME. *Measurement of Fluid Flow in Pipes Using Orifice, Nozzle, and Venturi.* ASME MFC-3M-1989. ASTM, 1990.

ASTM International. *Standard Guide for Evaluating Metals for Oxygen Service*. G94-05. ASTM, 2014.

Beeson, Harold Deck, Sarah R. Smith, and Walter F. Stewart. *Safe Use of Oxygen and Oxygen Systems: Handbook for Oxygen System Design, Operation, and Maintenance*. ASTM International, 2007.

Bryner E, Ransom D, Bishop J, Coogan S, Musgrove G. Design of a Small Scale Gas Turbine for a Hybrid Propulsion System. ASME. Turbo Expo: Power for Land, Sea, and Air, *Volume 8: Microturbines, Turbochargers and Small Turbomachines; Steam Turbines* ():V008T23A011. doi:10.1115/GT2015-42770.

Cunningham CS, Ransom D, Wilkes J, Bishop J, White B. Mechanical Design Features of a Small Gas Turbine for Power Generation in Unmanned Aerial Vehicles. ASME. Turbo Expo: Power for Land, Sea, and Air, *Volume 8: Microturbines, Turbochargers and Small Turbomachines; Steam Turbines* ():V008T23A021. doi:10.1115/GT2015-43491.

European Industrial Gases Association AISBL. *Oxygen Pipeline and Piping Systems.* IGC Doc 13/12/E. EIGA, 2012.

NASA. *Safety Standard for Oxygen and Oxygen Systems: Guidelines for Oxygen System Design, Materials Selection, Operations, Storage, and Transportation.* NSS 1740.15. NASA, 1996.

Nihart, G. J. and C. P. Smith. *Compatibility of Materials with 7500 psi Oxygen.* Union Carbide Corporation, Linde Division, 1964.

Stoltzfus, Joel M., Jesse Dees, and Robert F. Poe. *Guide for Oxygen Hazards Analyses on Components and Systems.* NASA Technical Memorandum 104823. NASA, 1996.